Author/s:
Weeratunge, H;Aditya, GR;Dunstall, S;de Hoog, J;Narsilio, G;Halgamuge, S

Title:
Feasibility and performance analysis of hybrid ground source heat pump systems in fourteen cities

Date:
2021-11-01

Citation:
Weeratunge, H., Aditya, G. R., Dunstall, S., de Hoog, J., Narsilio, G. & Halgamuge, S. (2021). Feasibility and performance analysis of hybrid ground source heat pump systems in fourteen cities. Energy, 234, https://doi.org/10.1016/j.energy.2021.121254.

Persistent Link:
https://hdl.handle.net/11343/339450

Feasibility and performance analysis of hybrid ground source heat pump systems in fourteen cities

Hansani Weeratunge[d,*], Gregorius Riyan Aditya[a], Simon Dunstall[c], Julian de Hoog[d,b], Guillermo Narsilio[a], Saman Halgamuge[d]

[a] *Department of Infrastructure Engineering, The University of Melbourne, Parkville, Australia*
[b] *IBM Research Australia, Melbourne, Australia*
[c] *CSIRO Data61, Docklands, Australia*
[d] *Department of Mechanical Engineering, The University of Melbourne, Parkville, Australia*

Abstract

Ground source heat pump systems (GSHP) for residential building heating, cooling and hot water are highly energy efficient but capital intensive when sized for peak demands. The use of supplemental sources of energy with GSHP systems, enables improved life-cycle economics through reduction in the size and cost of the GSHP components. This paper investigates the life-cycle economics of hybrid solar-assisted ground source heat pump systems (SAGSHP) using simulations validated from field data. The economics and optimal sizing of SAGSHP systems for heating dominant climates in four locations in Australia and ten locations elsewhere are evaluated in order to explore the suitability and relative merits of SAGSHP systems in a range of heating dominant climates. In locations having high or moderate levels of solar irradiation, high electricity prices, and high or moderate gas prices, SAGSHP systems are shown to have the lowest life cycle cost amongst alternatives, with predicted savings of up to 30%.

Keywords: Ground source heat pumps, Solar thermal, Hybrid systems, Life cycle cost, Optimisation

*Corresponding author
Email address: hansaniweera@gmail.com (Hansani Weeratunge)

Nomenclature

A	Area (m^2)
C	Cost ($)
Cp	Specific heat capacity ($JK^{-1}kg^{-1}$)
E	Electric power (W)
I	Solar irradiation (Wm^{-2})
L	Borehole depth (m)
m	Mass flow rate (kgs^{-1})
Q	Heat exchanged (W)
r	Radius (m)
R	Thermal resistance (mKW^{-1})
T	Temperature (^oC)
T_t^g	Average temperature of the ground at the borehole wall at time t (^oC)
U	Overall heat transfer coefficient ($WK^{-1}m^{-2}$)
V	Volume (m^3)
α	Thermal diffusivity of the ground (m^2s^{-1})
ρ	Density ($kg\ m^{-3}$)
η	Efficiency
λ	Thermal conductivity of the ground ($WK^{-1}m^{-1}$)

Array Variables and subscripts

a	Atmosphere
b	Borehole
g	Ground
hp	Heat pump
in	In
out	Out
s	Storage system
solar	Solar system
t	Time

1. Introduction

A significant percentage of global energy consumption is due to the heating, cooling and hot water systems of the building sector; as a result, the potential use of cost effective and renewable energy systems have gained increased attention. Among these, Ground Source Heat Pump (GSHP) systems have a high annual average efficiency and lower carbon emissions when compared with conventional systems. A heat pump driven by electricity enables GSHP to use the ground as a heat source in winter and a heat sink in summer. The heat is exchanged with the ground using a Ground Heat Exchanger (GHE) which circulates fluid through pipes built into building foundations, in horizontal trenches or in vertical boreholes [1]. Vertical boreholes are more common in urban areas due to the reduced land requirement.

GSHP systems have a long life expectancy ranging from 20–40 years. However, the underground

soil temperature will gradually be affected over long term operation if the annual heat extraction, and rejection are not balanced. The ground temperature might rise or drop in the long run, reducing the performance and efficiency of the system. This challenge can be overcome by integrating the GSHP system with a supplementary heat source or heat sink thus forming a *hybrid* GSHP system. In heating dominant climates, solar thermal energy is an auxiliary heat source which can be utilized to combat the annual energy imbalance. However, due to the intermittent nature of solar energy, thermal storage can enhance the reliability of the overall system. In heating-dominant climates GSHP systems that are designed to satisfy the peak demands (which might occur only for a few days per year) may also require an unduly large GHE (i.e., an excessively large total length of pipe embedded into the ground through boreholes). This degrades the system economics due to the high drilling cost of the boreholes. The hybrid GSHP approach has additional advantage that the ground heat exchanger can be designed to supply the base load of the energy demand, and a supplemental system such as solar thermal collection and storage, can supply the remainder, leading to a system with lower capital cost and better economy overall.

2. Approaches to the Optimised Design of GSHP Systems

An optimised GSHP system may provide substantial economic benefits over gas heaters, air source heat pumps (ASHP) and other conventional systems. Shonder *et al.* conducted a comparison between GSHP and conventional systems for a school building in Nebraska. The study considered Life Cycle Cost (LCC) contributions from installation, annual recurring energy and maintenance costs. The results showed that the GSHP system had a LCC 13% lower than the next most economic option [2].

Studies have been reported which analyse hybrid GSHP systems in different configurations to achieve efficient and economic solutions.Dickinson *et al.* studied the cost-effective sizing of a bivalent heating and cooling system comprised of a GSHP system and a conventional system in the UK, and found that the optimal hybrid GSHP system resulted in a 60% of capital cost reduction compared to a peak sized GSHP [3].

Furthermore, many studies have explored potential benefits of combining solar thermal collectors with heat pumps [4, 5, 6, 7]. Chiasson *et al.* analysed a GSHP system coupled with solar collectors as a retrofit HVAC system for a school building and reported a payback period of less than 10 years. The integration with solar thermal collectors was shown to reduce the size of the ground heat exchanger by 34% [8].

Farzin *et al.* compared the performance of a hybrid GSHP system with solar thermal collectors and a conventional GSHP system for a house in Milton, Canada. Results indicated that adding optimally sized solar collectors have reduced the ground heat exchanger length by 15%. Furthermore, the analysis has also shown an economic benefit of 8% for a 20 year life span [6].

Designers of building energy systems have several conventional options including air source heat pumps and, electric and gas heaters available for them. Many studies have tried to establish and quantify the economic benefits of GSHP systems over such conventional systems. Typically, LCC is used to evaluate the system as it considers all the costs related to installation, maintenance, replacement and operational cost through out the system life span. Biglarian *et al.* [9] compared the feasibility of a SAGSHP system, a GSHP system, a natural gas heater and an ASHP system for north western Iran. The analysis shows that the natural gas heater has the lowest LCC while a SAGSHP system is more financially attractive than a GSHP or ASHP system over a 20 year lifespan. It was found that a SAGSHP system has a discounted payback period of 8.6 and 12.1 years compared to GSHP and ASHP respectively (with a discount rate of 3.2%). Nouri *et al.* compared three different configurations of SAGSHP systems with a standalone GSHP and conventional system. It was found that the optimal SAGSHP system has a payback period of 13 years compared to the conventional system that uses natural gas for heating and electricity for cooling. When an equivalent cost of the environmental effects of using fossil fuels and natural gas exporting income for conventional system is considered, the payback period of SAGSHP system is further reduced to 6 years [10].

Energy savings and environmental criteria including carbon emissions are some of the non-financial indicators considered in feasibility studies of energy systems [11]. Various site-specific factors influence the performance of these systems. Michopoulos *et al.* illustrated how residential building topology affects the energy, environmental and economic benefits of GSHP systems in Cyprus [11]. Girard *et al.* analysed the performance of SAGSHP systems in 19 European cities with different levels of solar radiation and climatic conditions, and found that they are best suited for locations with cool climate and high solar radiation [5]. Stuart *et al.* evaluated the feasibility of GSHP systems for several locations and concluded that they are more economically advantageous when the price of electricity is low [12].

Optimising the size of the solar collector area and the depth of the borehole (i.e., total GHE field length) in SAGSHP systems is essential because of their influence on cost and therefore the competi-

tiveness with alternative systems. Mixed integer linear programs (MILP), Genetic Algorithms (GA) and evolutionary algorithms are some of the optimisation techniques that have been used to optimise energy system designs [13]. Somil *et al.* developed a bi-level multi objective optimisation algorithm consisting of a GA and MILP to optimise SAGSHP design and operation [14]. MILP is a convenient method for optimisation however the mathematical models of system components are often compromised in order to yield a linear optimisation problem. Furthermore, MILP typically provides 'perfect lookahead' of time-evolving supply and demand. This leads to underestimates of the operational costs of the system. The use of GA and other non-linear optimisation methods are therefore more common. Dynamic simulations and energy simulation tools such as TRNSYS [15] are also widely used in those studies [16, 17]. Nam *et al.* analysed the performance of a GSHP coupled with solar thermal storage for varying collector area, grout material and weather conditions using simulations. It was found that the heat exchange rate and the COP of the SAGSHP has improved 28.1% and 9.3% respectively, compared to GSHPS [16].

Lei *et al.* addressed the cost-optimal design of a SAGSHP system using a GA, and also applied an ANN model to data obtained from the simulation tool TRNSYS so as to predict the performance of the system [18]. However, a disadvantage of such methods is that it is mathematically infeasible to proving that the solutions obtained are close to global optima [13].

HVAC systems can be modified during the working life of the equipment, particularly if the original design explicitly considers and facilitates future changes and augmentations. The assessment of such flexibility requires financial modelling to make future decisions based on new information. Real Options Valuation (ROV) enables evaluation of the value that can be unlocked over a sequence of future decisions in an uncertain environment [19]. A common ROV technique, Regression MC, uses randomised (Monte Carlo, MC) simulations to generate a large number of feasible scenarios of uncertain parameters and then uses least squares linear regression to optimise the expected return and to determine a policy for future decisions that depend on the emergent system states [20]. When considering design optimisation for SAGSHP we can use ROV to assess future incremental system augmentations possibly made in response to evolving costs and demand, and through this identify a system design that optimises the expected return and is robust to uncertainties.

This paper addresses the optimisation of the borehole depth and the solar collector area of SAGSHPs to minimise the expected lifetime cost. Prior studies in the literature have explored this question but

only a subset assimilate real-world system performance data and validate against it, and none have investigated the additional financial benefits of systems that can be modified during their economic life in response to changing conditions. In this paper, flexibility via the future addition of solar collector area is incorporated. We use simulation for the assessment of SAGSHP candidate designs. This avoid compromises in the mathematical model that may be needed for linearization, and is in keeping with a ROV framework for valuing flexibility. Our simulation models are validated relative to data obtained from a SAGSHP system installed in Melbourne, Australia, extending a prior study [21]. The analysis is then propagated to 14 geographical locations with different climatic and economic conditions, to prove the suitability of the methods and to give insight into SAGSHP system designs and relative merits in a range of heating and cooling scenarios.

3. SAGSHP System Models and Experimental Validation

The operation and performance of a SAGSHP system depends on the type of components (GHE, solar thermal collector, thermal storage) and its configuration. The schematic diagram in Figure 1 shows the hybrid SAGSHP system considered in this study that consists of a vertical ground heat exchanger, heat pump, evacuated tube solar thermal collectors, thermal storage tank, a conventional electric heater and a gas booster for hot water. There are multiple possible ways of configuring SAGSHP systems targeting different climatic conditions, some of which are covered in the literature; we use here one of the mostly used configurations. We simulate the SAGSHP system using a mathematical model reported in [22] which was developed using data obtained from the field [23, 24]. In the field experiment, temperatures and the flow rates of the circulation fluid were measured using negative temperature coefficient thermistors and flow meters respectively. In addition, power consumption of the heat pump was measured by a power meter. Data was collected in five minute intervals over sixteen months. Further details of the experimental set up is presented in the Appendix.

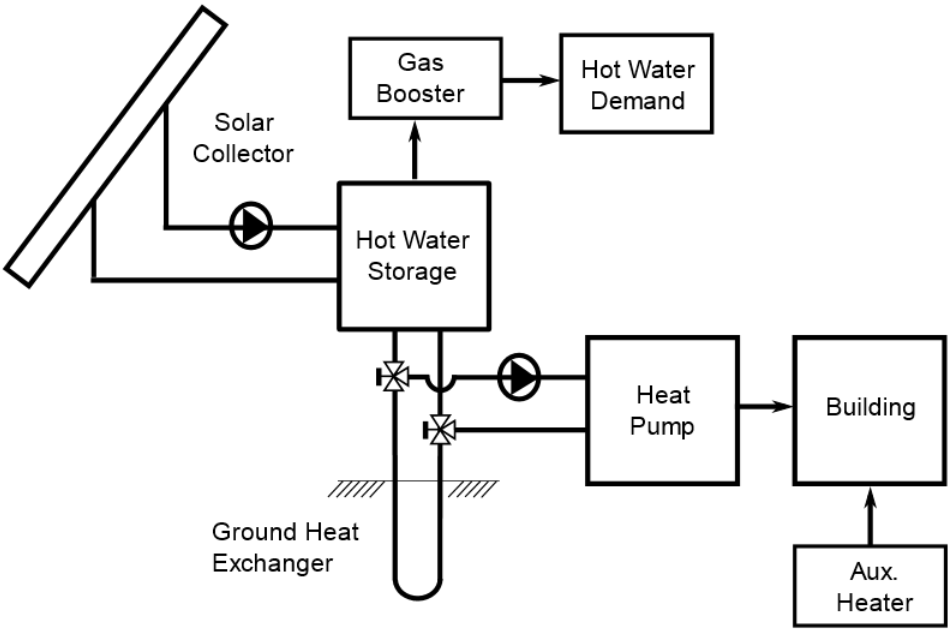

Figure 1: Hybrid solar assisted ground source heat pump system configuration for space heating, cooling and hot water

The control strategy used in the operation of the system is presented in Figure 2. In heating mode, the heat pump uses either the thermal storage tank or the ground as the heat source depending on their temperatures. If the temperature of the thermal storage tank exceeds the temperature of the ground by 5^oC, then the heat pump uses the tank as the heat source. The auxiliary heater is used only when the temperatures of both ground and thermal storage tank reach their minimum allowed temperatures.

When the temperature of the tank exceeds the maximum allowed Entering Water Temperature (EWT) of the heat pump (i.e. 30^oC) during days with high solar intensity, the energy from the solar collector is directed to hot water production. During summer, the cooling demand is fully met by the heat pump using the ground source as the heat source while the solar collectors are entirely used to produce hot water. The daily domestic hot water demand (calculated from the annual usage) has been considered instead of a demand profile since the domestic hot water demand depends on the occupants behaviour. An additional gas booster is considered to supply the hot water demand for the days with low solar intensity.

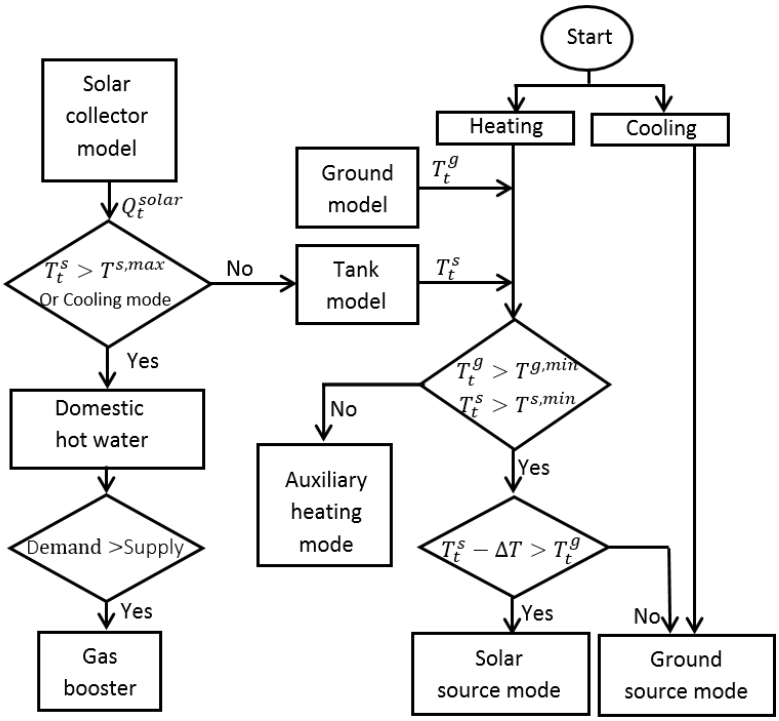

Figure 2: Operation of the hybrid solar assisted ground source heat pump system

In the following we describe the mathematical models used for the simulation studies reported in this paper, which are common to [22] where the focus was on operational control, and compare model and field-collected data for validation purposes.

An important measure used to assess the performance of heat pumps is the Coefficient of Performance (CoP), which is the amount of output energy ($Q^{hp,out}$) for one unit of electricity consumed (E^{hp}):

$$CoP = \frac{Q_t^{hp,out}}{E_t^{hp}}. \tag{1}$$

The CoP of a heat pump for a given flow rate is a linear function of the EWT which is typically provided in the manufacturers data sheet. The CoP can be calculated from the following equation where a and b are constants, and $T^{hp,in}$ is the temperature of the water entering to the heat pump (EWT):

$$CoP_t = a + bT_t^{hp,in}. \tag{2}$$

Figure 3 represents the distribution of the experimentally measured CoP variation with EWT. The central mark on each blue box represents the median, and the upper and lower edges indicate quartiles. The extreme data points are plotted individually using the colour red. For temperatures between 8-14.5 degrees the CoP for this heat pump can be represented as a linear function of the EWT.

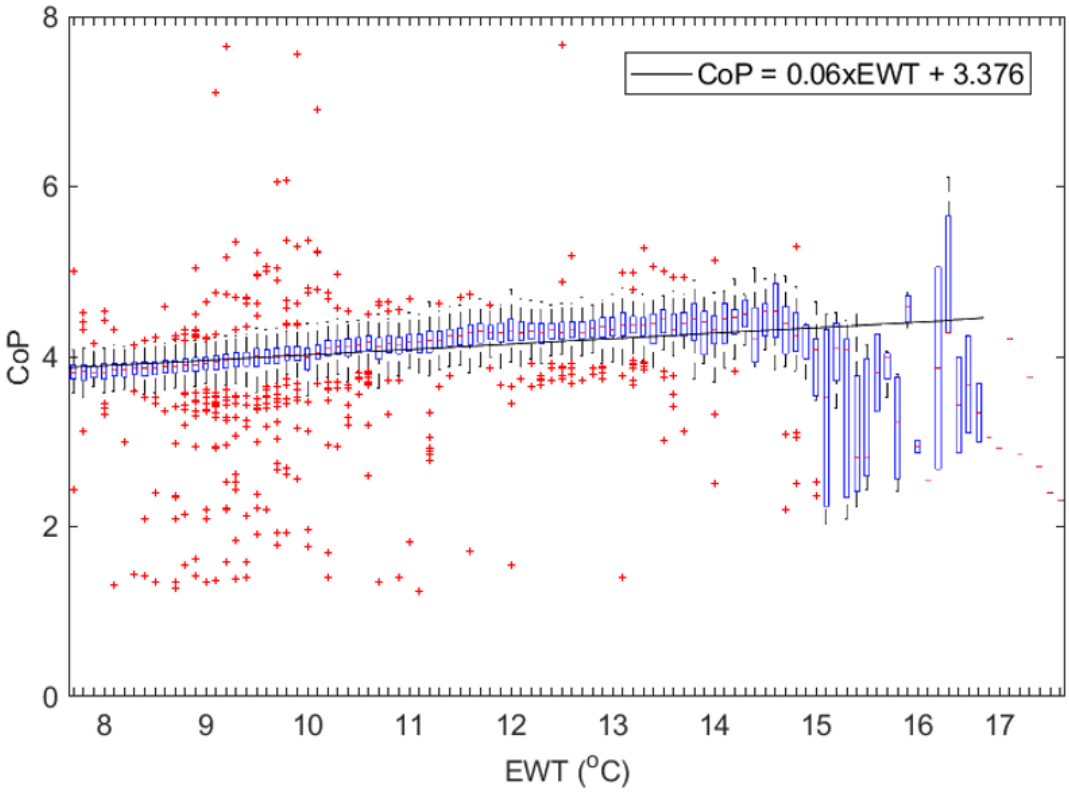

Figure 3: Distribution of experimentally measured CoP for a location in Melbourne

The demand of the building is expressed in Equation 3 where the total demand must be satisfied by $Q_t^{hp,out}$ (energy supplied by the heat pump) and Q_t^{aux} (energy delivered by the auxiliary heater).

$$Demand = Q_t^{hp,out} + Q_t^{aux} \tag{3}$$

A vertical borehole heat exchanger is considered in this study. Pipe U-loops are inserted into boreholes drilled to several tens of metres beneath the surface, and water or an anti-freeze solution is circulated in the U-loops to transfer heat from to to the ground. The design of the ground heat exchanger is influenced by energy demand and ground thermal characteristics. The drilling cost typically accounts for half of the total cost of small residential GSHP systems.

The average ground temperature alteration at the borehole wall ΔT^g with the rate of heat extraction and rejection q^g can be modelled using (4) by approximating the thermal load to a piecewise constant function where λ, α, L, rb, are the ground thermal conductivity, ground thermal diffusivity, borehole depth and radius respectively. This model was developed based on the Ingersoll and variable line heat

source model, one-dimensional heat transfer model and a steady-state heat pump model [25].

$$\Delta T_t^g = \frac{1}{4\pi\lambda L}\left[\sum_{j=1}^{N-1}(Q_{j+1}^g - Q_j^g)EI\frac{r_b^2}{(4\alpha\Delta t(N-j))}\right]; t = N\Delta t. \tag{4}$$

The temperature of the ground at the borehole wall can be estimated using (5), where T_0^g is the undisturbed ground temperature:

$$T_t^g = T_0^g - \Delta T_t^g. \tag{5}$$

The temperature of the circulation fluid at the outlet of the ground heat exchanger, which is the EWT to the heat pump, is modelled using (6), where R_b is the borehole resistance, m is the mass flow rate, and C_p is the specific heat capacity of the circulating fluid:

$$T_t^{g,out} = T_t^g - (\frac{R_b}{L} - \frac{1}{2mC_p})Q_t^g. \tag{6}$$

The variation of the simulated and the actual measured temperatures for the ground temperature at the borehole wall and the EWT are presented in Figures 4 and 5 respectively. Actual heat transferred to and from the ground are approximated as piecewise constants, and the geometrical and thermal properties of the ground heat exchanger were assumed to be homogeneous. These parameters obtained from a thermal response test conducted on the site have been considered as the inputs for the simulation. Furthermore, in the calculation of the EWT, the pipes to the heat pump have been assumed to be perfectly insulated and therefore the heat losses from the pipes have been neglected. This assumption seems reasonable because the theoretical values correspond well with the experimental data as shown in Figures 4 and 5.

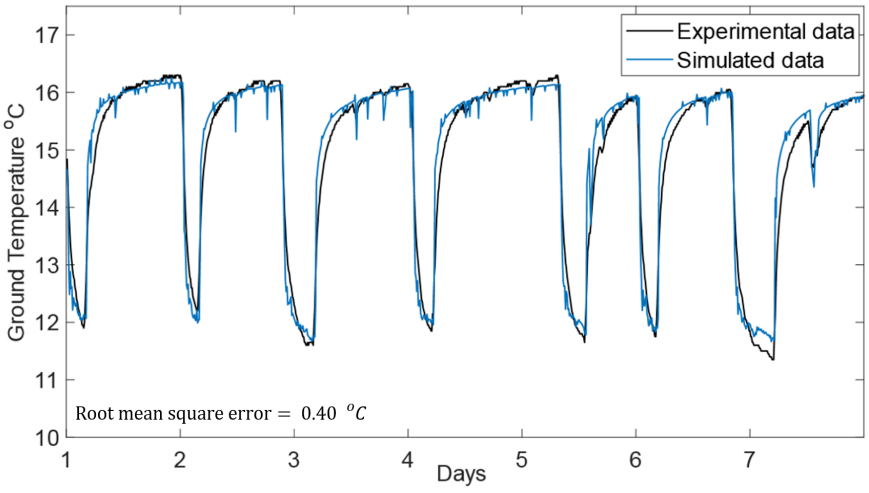

Figure 4: Comparison of the ground temperature between experimental and simulated data for Melbourne

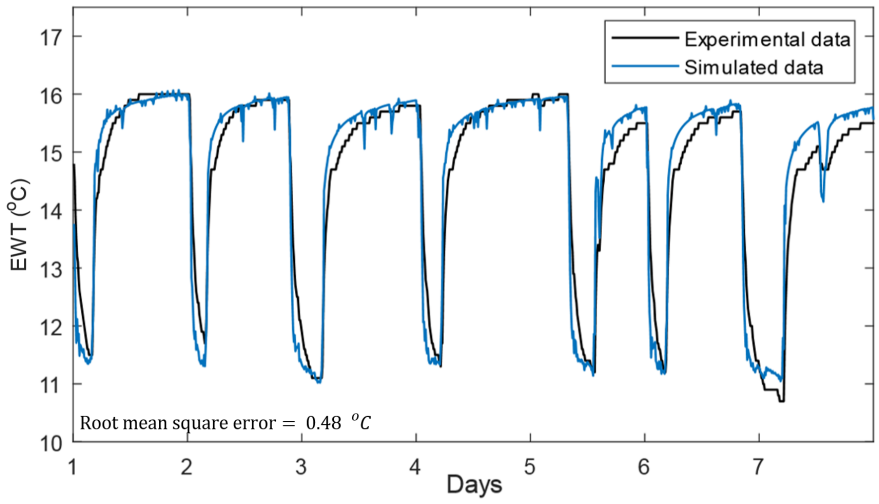

Figure 5: Comparison of the Entering Water Temperature (EWT) between simulated and experimental data for Melbourne

Solar thermal collectors can be utilized in the production of hot water and in space heating. Most solar water heating systems are comprised of a solar collector, a thermal storage tank and an electric or gas booster.

The efficiency of a solar collector (η^{solar}) typically depends on various factors such as the type and the configuration of the collector, the hydraulic connection, the circulation fluid, heat exchanger type, solar collector temperature, ambient temperature and the solar radiation flux reaching the collector. Many studies in literature present the efficiency of collectors as a function of some of these parameters [26], but in this study the efficiency is approximated to a constant value, as in [27, 28]. However, a detailed study may be carried out in future taking these factors into consideration as it not only affects the efficiency, but also the initial cost of the system.

The useful solar thermal energy Q^{solar} can be then calculated using (7) where A^{solar} and I_t are the area of the collector and the solar irradiation at time t respectively:

$$Q_t^{solar} = A^{solar} I_t \eta^{solar}. \tag{7}$$

The energy balance of an insulated thermal storage tank has been modelled according to (8) assuming that the stored water has a uniform temperature profile. Euler method has been used to discretise the temperature of the thermal storage. The accuracy of the model can be increased by reducing the time step size. However, half hour or hourly time intervals have been widely considered in research to reduce the computational efforts required [29, 30].

V^s, ρ, C_p, U, A^s, T_t^s and T_t^a are the tank volume, density of the fluid, specific heat capacity, coefficient of heat loss, external surface area of the tank, temperature of the tank at time t and temperature of the atmosphere at time t, respectively.

$$V^s \rho C_p \frac{T_t^s - T_{t-1}^s}{\Delta t} = Q_t^{solar} - Q_t^{s,out} - UA^s(T_t^s - T_t^a). \tag{8}$$

When the heat pump utilises the thermal storage tank as the heat source, the temperature of the tank has been considered as the EWT assuming the pipes are perfectly insulated. Figure 6 plots measured and simulated tank fluid temperature T_t^s over a period of one hour. The inputs for the simulations are Q_t^{solar},T_t^a, $Q_t^{s,out}$, V^s, ρ, C_p,U and A^s. These parameters are part of manufacturers' specifications except for Q_t^{solar}, T_t^a and $Q_t^{s,out}$. Q_t^{solar} is calculated from (7) using solar irradiation data I_t obtained from weather observations. T_t^a is directly measured using temperature sensors. Energy balance is used in the computation of $Q_t^{s,out}$, via (9) where m_t, $T_t^{s,out}$ and $T_t^{s,in}$ are the flow rate, outlet and inlet temperatures at the outlet loop of the tank:

$$Q_t^{s,out} = m_t C_p (T_t^{s,out} - T_t^{s,in}). \tag{9}$$

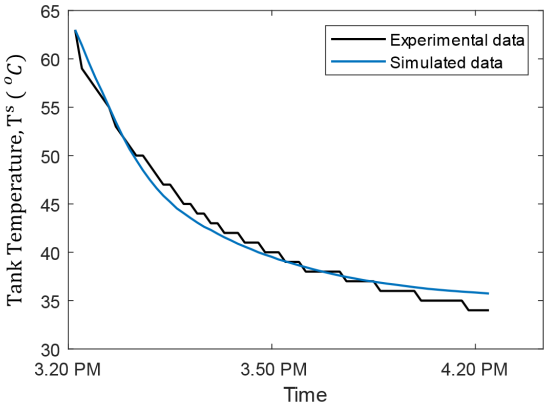

Figure 6: Variation of thermal storage tank temperature T^s for a location in Melbourne

4. Evaluation of SAGSHP for Melbourne, Australia

Simulations were carried out to explore the performance of the SAGSHP system with varying borehole depths and solar collector areas in Melbourne, Australia, where residential applications are typically heating-dominant.

A system with a maximum capacity of 10kW is considered (i.e. a peak demand of 10kW). System operation in half-hourly intervals was simulated in order to obtain the annual energy consumption and to explore system performance. The annual demand to be satisfied by the system is assumed to be the same throughout the life span of the system. The project life is considered to be 20 years [31] and costs are presented in Australian dollars throughout this paper. (At the time of writing (August 2019) 1 AUD is equivalent to 0.68 USD)

LCC analysis takes into account the costs involved in the system over the entire project life. A simple LCC can be expressed as the summation of installation cost C_{int}, operational cost C_{op}, and the replacement cost C_{rep}. We consider the Net Present Value (NPV) of these costs over the 20 year period. NPV is the current value of future cash flows as is calculated using (10) where N, C_k, and i are the project life, cash flow of year k, and effective interest rate or minimum attractive rate of return:

$$NPV = \sum_{k=1}^{N} \frac{C_k}{(1+i)^k}. \tag{10}$$

Cost data for residential properties in Melbourne was collected by the Sustainable Shallow Geothermal Energy Research and Demonstration Project under the Sustainable Energy Pilot Demonstration Program and it has been considered as the basis for this study [31]. In addition, a detailed description of the lifespans, costs of the system, and the economic indicators used in this study can be found in [31].

Figures 7 to 10 plot the LCC, auxiliary energy use, average CoP and EER respectively for different borehole depths and solar collector areas. The optimal system design (minimum LCC) is achieved with a $70m$ borehole depth and $8m^2$ solar collector area as shown in Figure 7. For shorter borehole lengths the lower capital cost is outweighed by increased running costs attributable to greater use of auxiliary heating. For longer borehole depths, the LCC is increased by higher drilling capital costs. Solar collectors bring a reduction in LCC for shorter boreholes because the solar energy substitutes for auxiliary heater use, whereas the capital costs of solar are unfavourable when boreholes are deeper and GSHP are able to satisfy more of the peak demand. For the optimal system design 5.5% of the total energy demand is satisfied by the auxiliary heat supply as shown in Figure 8. The average CoP and the EER increase with borehole depth. Increased efficiency in both heating and cooling stems from larger boreholes being able to extract and reject more heat due to their increased heat capacity and the larger contact area of the ground being available for the GHE. The simulation results suggest that the CoP increases with solar collector area. Combining solar collectors with the heat pump increases the EWT of the heat pump. The

resulting high efficiency of the heat pump increases the overall CoP of the system. However, the EER of the system has slightly dropped during summer due to the addition of solar collectors that causes a long term increase in soil temperature.

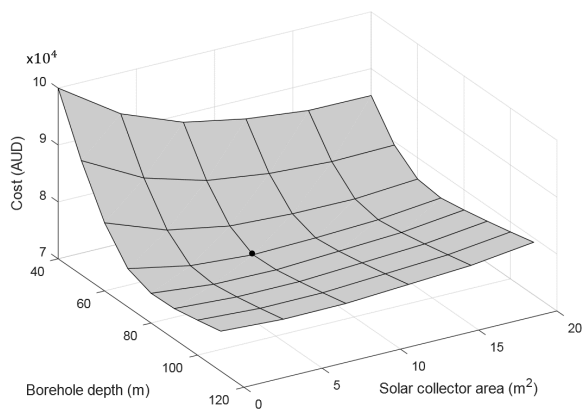

Figure 7: Variation of the LCC for Melbourne, Australia

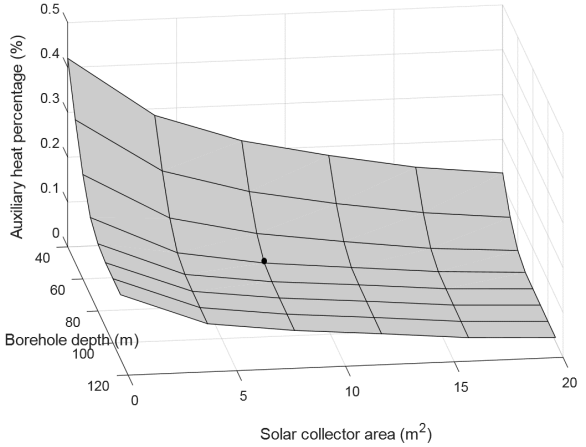

Figure 8: Percentage of auxiliary energy use

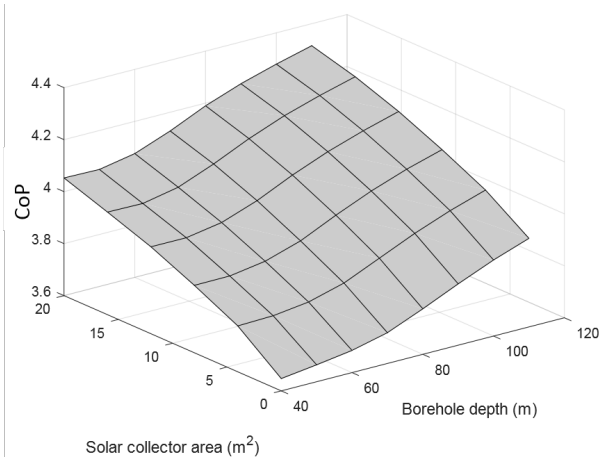

Figure 9: Variation of the CoP

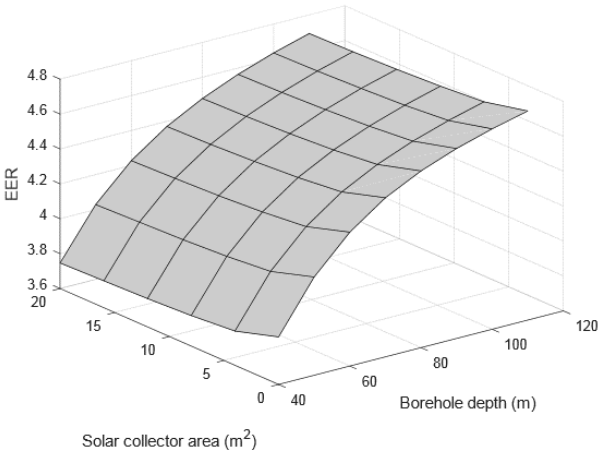

Figure 10: Variation of the EER

A system design that is optimised for a particular predicted energy price trajectory may not remain optimal if the realization of energy prices departs significantly from this forecast. Therefore, design changes to SAGSHP systems such as increasing the solar collector area need to be considered. Here, we consider the Real Option of increasing the solar collector area in future. Changing of the borehole depth is not considered due to the practical difficulty in increasing the depth once the GHE is installed. Future price changes of solar thermal collectors are neglected because as a technology they are mature and show only minor price variability and trend [32]. Our interest is in exploring whether the option of future system augmentation might be valuable if future energy prices deviate in a predictable way from a forecast. This is important given the uncertainties inherent in predictions of future energy costs. A

mean reversion process represented by (11) is used to model annual energy price increments: C is the price increment, γ is the mean reverting rate, σ is the volatility (standard deviation of the noise), and W^T is a Brownian motion.

$$\Delta C_t = \gamma(C_t^{mean} - C_t)\Delta t + \sigma C_t \Delta W^T(t) \tag{11}$$

For the ROV we used Monte Carlo simulations to generate multiple scenarios of energy prices using (11), randomised the control variable which is the solar collector area increase at each time step, and applied least squares linear regression to determine the optimal decision for each system state [20]. A 20 year horizon was considered and it is assumed that the system augmentation choice was available to the decision maker once a month. For the moderate level of energy price uncertainty captured by a mean reverting process with realistic parameters, the ROV analysis showed that the optimal initial system design (collector size and borehole depth) could not be improved upon by first installing a system with fewer solar collectors and then waiting to observe future energy prices. Furthermore, at any future time the optimal system for the remainder of the time horizon remained the same as initial optimal system. This null result we suggest stems from the assumption of mean reversion in the energy price, and from the rather shallow gradient in LCC around the optimal design leading to the advantages from early-period operational cost savings from a larger solar collector array outweighing the likelihood-weighted avoided capital savings. If we were to admit the possibility of larger and irreversible energy price changes, then system augmentation may become favourable. However, such trajectories would be speculatively proposed with little or no supporting evidence.

4.1. Comparison with conventional systems

The simulated performance of a hybrid SAGSHP system (System 1) of the optimally-sized design identified above is compared to predictions for the following three heating and cooling systems:

- System 2: (GSHP) - GSHP system, with an auxiliary electric heater and instantaneous gas hot water. The LCC of GSHP systems is plotted in Figure 7 corresponding to a solar collector area of zero. The system designs with the lowest LCC are used for the comparison exercise. In both SAGSHP and GSHP cases these are hybrid systems.

- System 3: (ASHP) - Reversible Air Source Heat Pump (ASHP) with instantaneous gas hot water. ASHP systems require less capital cost compared to GSHP systems and have a relatively high

energy efficiency.

- System 4: (ASHP+Gas) - Combination of cooling only ASHP and gas furnace with instantaneous gas hot water. Gas furnaces are low cost to install and can be economically effective in heating dominant climates. An ASHP is used to fulfil cooling requirements during summer.

Figure 11 illustrates the breakdown of the LCC including the investments and the operation cost for these systems. The investment cost consists of the installation and the replacement costs of the components. The operation cost for the Systems 3 (ASHP) and 4 (ASHP+Gas) is calculated based on annual heating and cooling demand and approximating the efficiencies of all the components as constants. A detailed discussion of the installation costs and other economic parameters of the systems considered in this study can be found in [31]. According to Figure 11, hybrid SAGSHP system has the highest investment cost compared to other systems. However, it has the lowest operating cost, making it overall the most economic system. Operation costs added over the 20 year lifespan of each proposed system are the dominant components of cost.

The energy consumption (i.e., electricity and gas) of the systems and their respective CO_2 emissions are shown in Figure 12. Melbourne has a relatively high electricity emission factor (EF) of 1.08 kg of CO_2 per kWh related to electricity consumption. This is due to a high percentage of coal in the energy mix of this region [33]. Reticulated natural gas has a lower EF compared to electricity, which is 51.4 kg of CO_2 per GJ (i.e., 0.185 kg of CO_2 per kWh). Accordingly, the highest CO_2 emissions are from the ASHP system as it has the highest electricity consumption compared to other systems, although this obviously changes if on-site electricity is utilised. The hybrid SAGSHP system has the lowest power consumption and the lowest CO_2 emissions, making it the best economic option and the best environmental option for Melbourne's current climate.

5. Impact of Different Climatic Conditions and Energy Costs Evident by the Results

To investigate the effect of different climatic conditions on performance, simulations were carried out for different geographical regions shown in Figure 13 with heating dominant climates since solar collectors coupled in SAGSHP are utilized as a supportive heat source. In addition to Melbourne, three other cities from Australia and ten cities from around the world with heating dominant climate and different ratios of annual heating to cooling load have been selected.

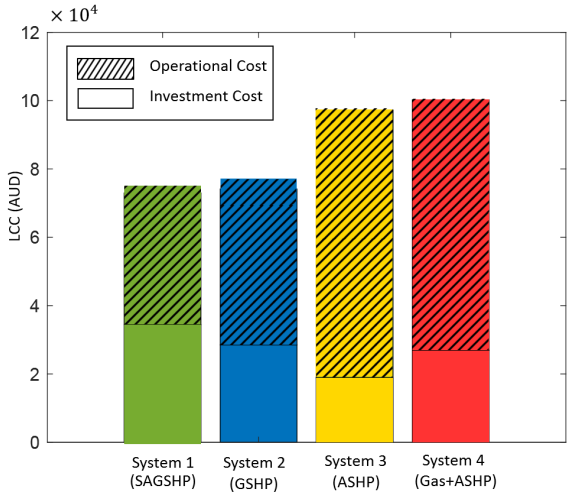

Figure 11: Cost comparison of the systems

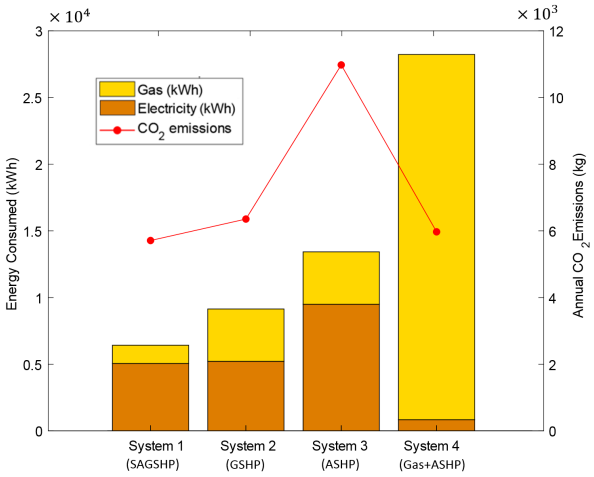

Figure 12: Annual power consumption and the CO_2 emissions

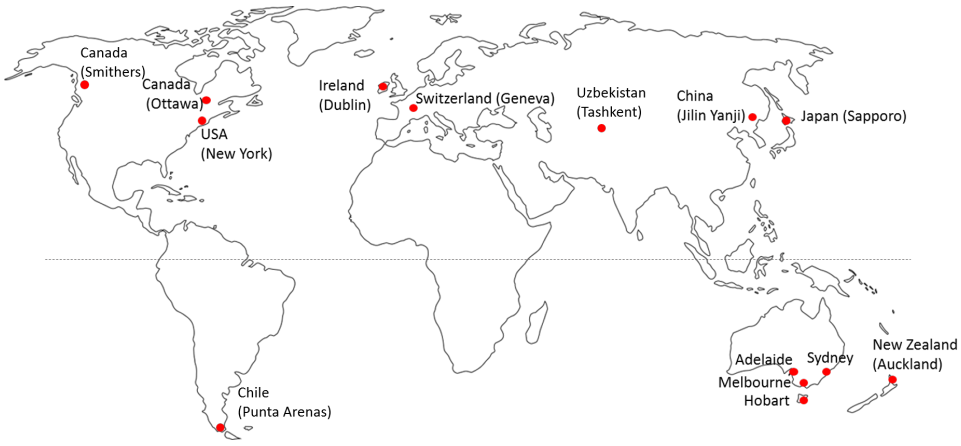

Figure 13: Range of selected climatic conditions including four Australian cities and ten cities in other countries

The annual atmospheric temperature and the solar radiation used in the simulations for the locations were obtained from EnergyPlus [34] which is an open source building energy simulation program.

The heating and cooling demand of the building is calculated using the bin method which is widely used in designing residential thermal systems [31]. In this method, the load profile was established by the peak load and the balance point temperatures. For the purpose of comparison, a peak load of 10kW is considered for all locations. It is assumed that no heating or cooling is required when the atmospheric temperature is above 18 ^oC during winter, and below 25 ^oC in summer as been used in previous studies [35, 36]. However, those balance temperatures could vary depending on the occupant's thermal sensation.

Table 1 presents an overview of the climatic conditions, average COP of ASHP, retail prices of electricity and gas, and the CO_2 emission factor of electricity for each of the 14 locations [37, 38, 39, 40]. LCC of the system may depend on location specific factors such as economic indicators, geological conditions and labour costs. However, it is assumed that the parameters used in Table A.3 remain the same for all locations. Some of these parameters are common to all locations, and some other parameters are obtained from Melbourne due to practical difficulties. Furthermore, Subsidies and rebates that may be provided for renewable energy solutions including GSHP systems are ignored.

Table 1: Climatic conditions and parameters of the 14 locations

Location	Undisturbed ground temperature (^oC)	Annual heating demand (MWh)	Annual cooling demand (MWh)	Annual solar radiation (MWh/m^2)	Electricity price (AUD /kWh)	Gas price (AUD /kWh)	Electricity emission factor (CO_2 kg/kWh)	Average ASHP COP
Melbourne	16.7	17.7	2.1	1.47	0.28	0.10	**1.08**	2.06
Sydney	**20.4**	**9.6**	1.5	1.77	0.24	0.13	0.83	2.08
Adelaide	19	15.4	3.5	**1.81**	0.31	0.13	0.79	2.07
Hobart	14.5	24.7	0.2	1.39	0.20	0.13	0.14	2.01
Sapporo	10.8	24.8	0.8	1.17	0.36	**0.18**	0.46	1.80
Auckland	17.3	13.9	-	1.5	0.27	0.13	0.21	2.08
New York	14.1	18.7	2.7	1.45	0.17	0.05	0.59	1.86
Jilin Yanji	7.4	26.0	1.5	1.26	0.11	0.06	1.07	1.64
Dublin	11.6	24.3	-	**0.9**	**0.38**	0.11	0.57	1.95
Geneva	12.4	24.3	0.9	1.18	0.20	0.13	**0.003**	1.89
Ottawa	7.7	25.5	0.9	1.34	0.12	**0.04**	0.19	1.68
Punta Arenas	8.3	**39.1**	-	1.19	0.33	0.14	0.41	1.85
Tashkent	16.6	18.7	0.7	1.71	**0.04**	0.05	0.57	1.86
Smithers	**5.6**	23.5	0.2	1.09	0.12	**0.04**	0.19	1.71

Highest and lowest values are in bold

The LCC variation for the selected cities demonstrated three distinct patterns. Figures 14a, 14b and 14c are representations of each pattern where they provide insights to the LCC variations of both GSHP and SAGSHP systems. In this context, System 1 (SAGSHP) and System 2 (GSHP) are considered as hybrid GSHP systems.

- Consider Figure 14a (Jilin Yanji), the line with the collector area of zero (Red line) represents

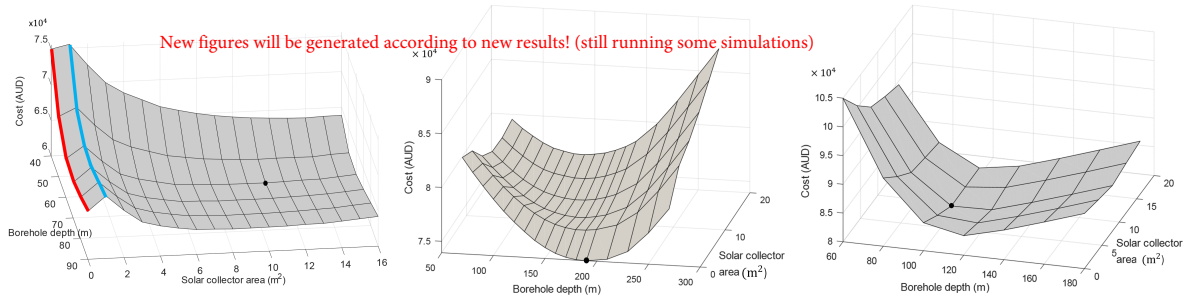

(a) Auckland (b) Jilin Yanji (c) Geneva

Figure 14: LCC variation with the borehole depth and the solar collector area for Auckland, Jilin Yanji and Geneva

the LCC of GSHP systems. Any system with a collector area greater than zero (anything except for the red line) represents SAGSHP systems. According to the figure, there are instances where the LCC of SAGSHP is greater than the LCC of GSHP systems. For example, the cost of the GSHP system (red line) is lower than the SAGSHP system with a collector area of $2m^2$ (blue line) due to the reduction of the costs involved in solar collectors. However, with the increased solar collector area, the LCC is further reduced reaching an optimal point for a specific borehole depth. For conditions in Auckland it is evident from Figure 14a that the optimal SAGSHP system is more economical than the optimally designed GSHP system. However, this also suggests that implementing a SAGSHP system could be more costly than a GSHP system if the optimal design parameters are not identified. Among the cities we selected for this study, Dublin and Punta Arenas follow a similar pattern to Auckland.

- For the climatic conditions in New York, the addition of solar collectors always increases the LCC of a SAGSHP system (Figure 14b). A GSHP system with a gas hot water system is cheaper than a SAGSHP for Jilin Yanji. Ottawa, Smithers and Tashkent also exhibit a similar pattern. The common factor among theses cities is that they have a lower gas price, enabling the operational cost premium of gas hot water production to be of a lower total value than the capital cost of solar collectors.

- Figure 14c represents the LCC of a hybrid SAGSHP system in Geneva which has a similar pattern to Melbourne. Several of the other selected locations (Auckland, Sapporo, Sydney, Adelaide, and Hobart) have also followed a similar pattern. For these locations an optimally-sized hybrid SAGSHP system has the lowest LCC.

The optimal design parameters of the systems and their CoP and EER for each location are presented in Table 2. These design parameters are uniquely determined by the climatic conditions and the undisturbed ground temperature for each location as shown in Table 1. It is evident from Table 2 that larger borehole depths are required for cities with high heating demands and low undisturbed ground temperatures. In addition, for locations where hybrid SAGSHP systems are more economical than hybrid GSHP systems, the collector area is determined by the availability of the annual solar radiation. For example, large solar collectors are required for locations with low annual solar radiation such as Punta Arenas and Dublin.

Table 2: Results of the optimal design for the 14 locations

Location	Optimal Design Parameters		Average CoP	Average EER	Optimal HVAC system
	Borehole Depth (m)	Solar Collector Area (m^2)			
Australia - Melbourne	70	8	3.95	4.37	SAGSHP
Australia - Sydney	50	8	4.0	4.16	SAGSHP
Australia - Adelaide	60	8	4.1	4.129	SAGSHP
Australia - Hobart	100	12	3.95	5.27	SAGSHP
Japan - Sapporo	160	16	3.89	5.57	SAGSHP
New Zealand - Auckland	60	12	4.08	-	SAGSHP
USA - New York	110	-	3.73	4.95	GSHP
China - Jilin Yanji	150	12	3.79	6.04	ASHP
Ireland - Dublin	130	12	3.88	-	SAGSHP
Switzerland - Geneva	130	8	3.80	5.46	SAGSHP
Canada - Ottawa	210	-	3.64	6.2	GAS+ASHP
Chile - Punta Arenas	250	16	3.89	-	SAGSHP
Uzbekistan - Tashkent	60	-	3.67	3.77	ASHP
Canada - Smithers	210	-	3.6	6.6	GAS+ASHP

Figure 15 compares the LCC of the systems for the 14 locations. Among all the systems, SAGSHP systems have the highest investment cost and the lowest operation cost for all the selected cities. Therefore, feasibility of a SAGSHP system for a particular location depends on the ability to offset its high installation cost with a low operation cost. Energy prices play an important role in determining this.

Optimally designed hybrid SAGSHP have the lowest LCC compared to other available options for 9 out of the 14 selected cities. One of the common factors of these cities is that they have a relatively high electricity cost compared to other locations. Therefore, having an efficient heating and cooling system would save more money compared to other conventional systems. The high capital cost involved

in SAGSHP system is outweighed by the lower operation cost over the system's life span.

A GSHP system with gas hot water is a better option than a SAGSHP system for locations with low gas prices. However, ASHP+Gas could also be the most ideal HVAC system for locations with very low gas prices. Therefore, the feasibility of GSHP system depends on the ability of outweighing the cost of ASHP+Gas system with efficient operation which results in a lower operational cost. For New York, GSHP system is the most economic solution among the systems due to reasons discussed above.

For locations with low electricity price, ASHP system is the most economical system among the other options. ASHP system has the lowest investment cost compared to other systems. Therefore, it is evident that SAGSHP or GSHP systems cannot offset their high investment cost for cities with low electricity price if lifetime investment is only considered for 20 years. Accordingly, for Tashkent and Jilin Yanji, ASHP systems are the most economical HVAC system due to their lower electricity prices.

Compared to other systems, a cooling-only ASHP system with gas furnace has the highest LCC for majority (9 out of 14) of the locations. The lower efficiency of gas furnaces compared to ASHP and GSHP is the main factor in the increased operation cost of the system. In addition, it has a higher investment cost compared to ASHP system. Therefore, these systems are less economic compared to other systems for location with high and moderate gas prices. However, for locations with very low gas prices, such as Ottawa and Smithers, these systems are the most cost effective HVAC system among the selected systems.

Figure 16 compares the LCC of the most economical hybrid GSHP system and the conventional system with solid line indicating when the costs are equal. Accordingly, for 10 cities out of 14, hybrid GSHP systems are economically more suitable than conventional HVAC systems. For Jilin Yanji and Tashkent, ASHP systems have the least LCC and, for Ottawa and Smithers, ASHP+Gas systems are the most economic HVAC system among the selected systems. However, for Jilin Yanji and Tashkent, hybrid ground source heat pumps would become cheaper than ASHP systems if the electricity prices of these cities increase to 0.19$ (72% increase) and 0.07$ (77% increase) respectively. On the other hand, for Ottawa and Smithers hybrid GSHP systems would become the most economic system if the gas price increases to 0.053$ (32% increase) and 0.062$ (55% increase).

Figure 17 represents the annual CO_2 emissions for systems in the selected cities assuming the use of grid-sourced electricity. SAGSHP systems have the lowest annual CO_2 emissions followed by GSHP

systems, except in Jilin Yanji where ASHP with gas furnace has the lowest emissions. In Jilin Yanji, SAGSHP, GSHP and ASHP systems have relatively high amounts of emissions due to the high emission factor incorporated with electricity generation. In contrast, Geneva, Auckland and Hobart have very low emissions for SAGSHP, GSHP and ASHP due to low electricity emission factors. As electricity systems become de-carbonized through displacement of fossil sources in future, the emissions favourability of the SAGSHP systems will increase.

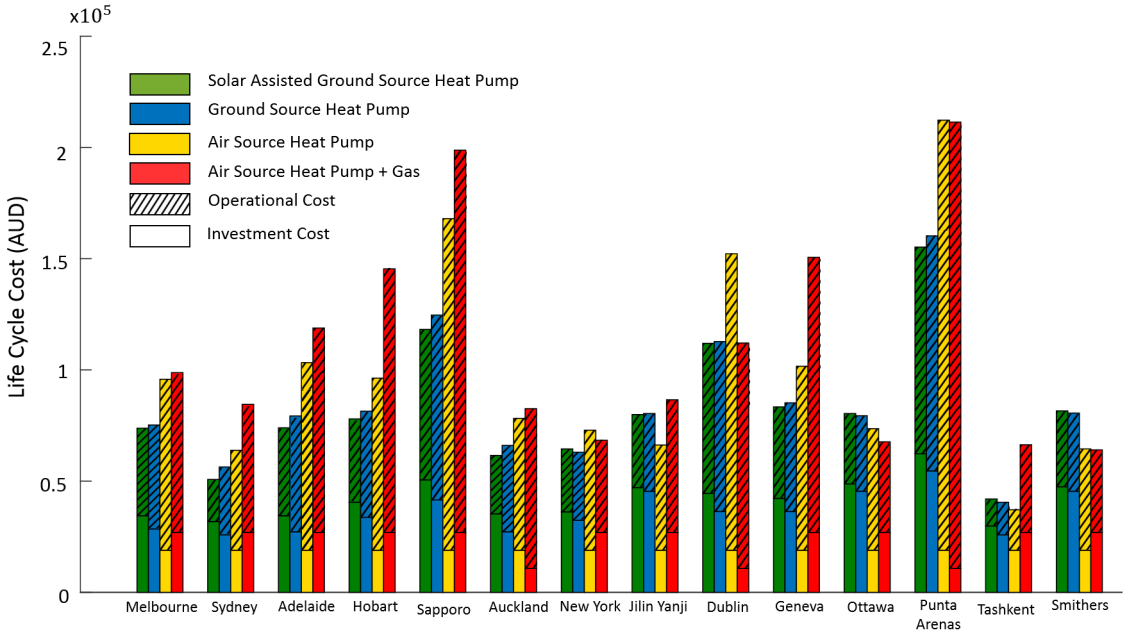

Figure 15: Comparison of the LCC between the selected HVAC systems

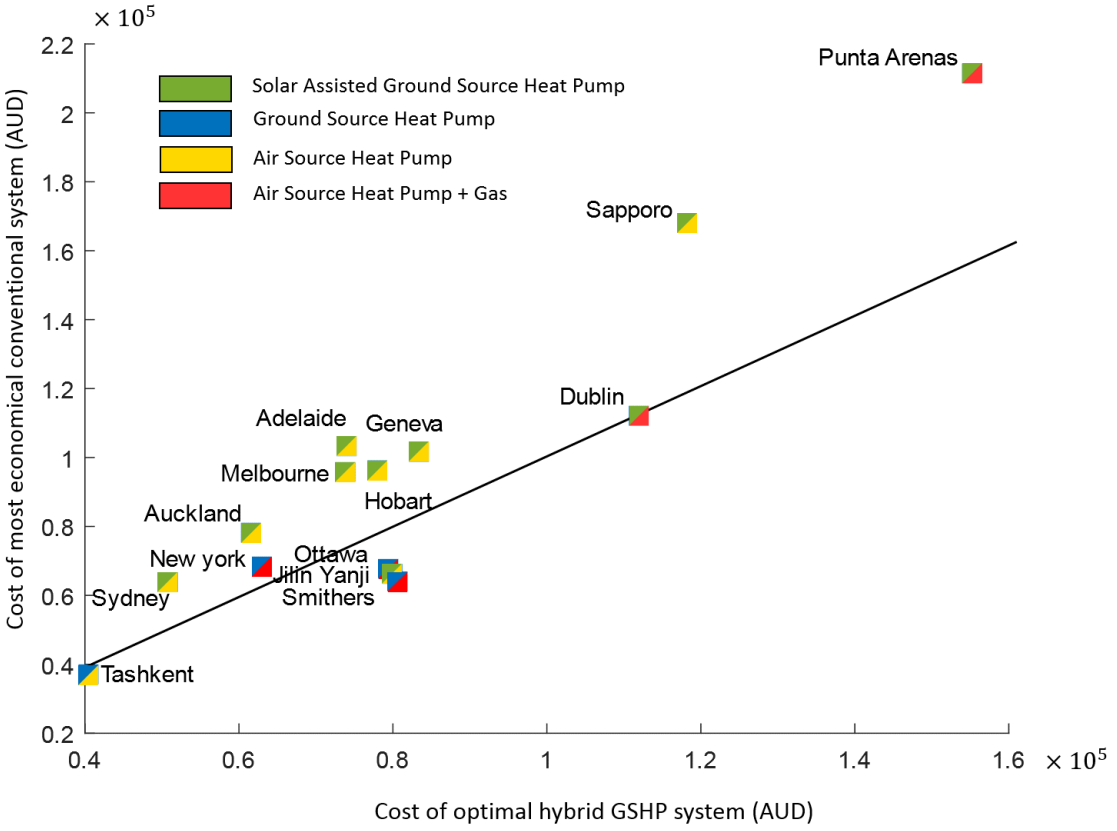

Figure 16: Cost comparison of the LCC between the optimal hybrid GSHP and the most economical conventional system

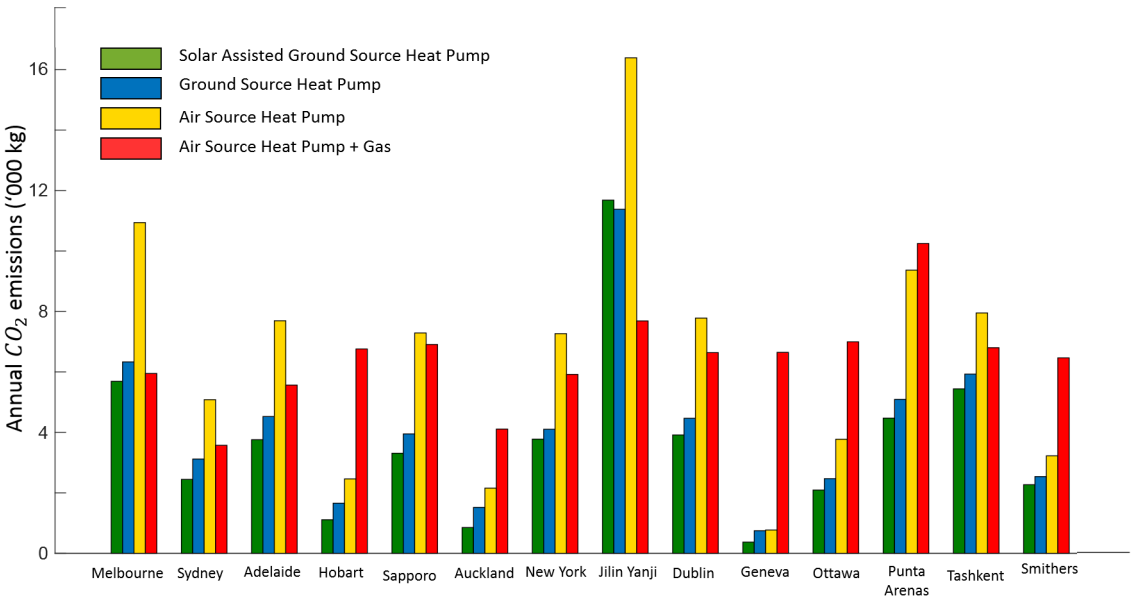

Figure 17: Annual CO_2 emissions

6. Conclusions

This study considers the optimal Life Cycle Cost of SAGSHP systems which can be used for heating, ventilation, air conditioning and hot water production. Simulations were carried out using a mathematical model that was developed in this study and then verified using data from a field experiment site located in Melbourne, Australia. A comparison to a hybrid GSHP system, reversible ASHP and a cooling only ASHP with gas furnace is also provided. Simulations and comparisons were carried out for 14 different locations to study the effect of the climatic conditions and different electricity and gas prices. Based on the results obtained in this study, we conclude:

- Designing a hybrid SAGSHP system to cover a proportion of the total heating demand of a building may be more economical than having a SAGSHP that can cover the total heating and cooling demand. Finding the optimal design parameters of the system design is important in reducing the economic life cycle cost of the system. In addition, the LCC of implementing a SAGSHP could be higher than a GSHP system if the optimal design parameters are not found.

- The design parameters of a SAGSHP system depend mainly on the climatic and geographic conditions of the location. Larger boreholes may be required for locations with high heating demand and low undisturbed ground temperatures, and larger solar collector areas are required for locations with low annual solar radiation.

- The favourability of a SAGSHP system depends mainly on whether it is possible to offset the high installation cost. Compared to conventional systems, SAGSHP systems are more economical for locations having a higher electricity prices, and high or moderate gas prices. An optimally designed hybrid GSHP system can achieve up to 30% LCC reduction compared to the next most economic conventional HVAC system. However, for locations with much lower gas prices, GSHP systems with an instantaneous gas hot water system are typically a more economically-favourable option compared to SAGSHP systems.

These results support the intuitive notion that when designing a hybrid SAGSHP system it is crucial that the design is optimised specifically for the site and that the economics of the system are evaluated over the lifespan of the system. In future work, the system will be evaluated for different types of GHEs, solar thermal collectors and thermal storages, as the system performance may vary for different types of

components. Furthermore, a more accurate model that considers a time varying efficiency will be used to model the performance of solar thermal collectors.

Acknowledgements

The contribution of the first-named author was supported by a Melbourne Research Scholarship and a CSIRO Data61 scholarship. The authors acknowledge the financial support for this project by the Victorian Government and ARC LP160101486, the property owners who permitted monitoring of their system, and Mr. Daniel Gaviria for the assistance provided with the field experiment site design and installation.

7. Reference

References

[1] I. W. Johnston, G. A. Narsilio, S. Colls, Emerging geothermal energy technologies, KSCE Journal of Civil Engineering 15 (4) (2011) 643–653. doi:10.1007/s12205-011-0005-7.

[2] J. A. Shonder, M. Martin, P. Hughes, J. Thornton, Geothermal heat pumps in k-12 schools: a case study of the lincoln, nebraska schools., US Department of Energy Publications, paper 30.

[3] J. Dickinson, T. Jackson, M. Matthews, A. Cripps, The economic and environmental optimisation of integrating ground source energy systems into buildings, Energy 34 (12) (2009) 2215 – 2222, eCOS 2007. doi:https://doi.org/10.1016/j.energy.2008.12.017.

[4] D. Carbonell, M. Haller, E. Frank, Potential benefit of combining heat pumps with solar thermal for heating and domestic hot water preparation, Energy Procedia 57. doi:10.1016/j.egypro.2014.10.277.

[5] A. Girard, E. J. Gago, T. Muneer, G. Caceres, Higher ground source heat pump cop in a residential building through the use of solar thermal collectors, Renewable Energy 80 (2015) 26 – 39. doi:https://doi.org/10.1016/j.renene.2015.01.063.

[6] F. M. Rad, A. S. Fung, W. H. Leong, Feasibility of combined solar thermal and ground source heat pump systems in cold climate, canada, Energy and Buildings 61 (2013) 224 – 232. doi:https:

//doi.org/10.1016/j.enbuild.2013.02.036.
URL http://www.sciencedirect.com/science/article/pii/S0378778813001126

[7] P. Eslami-nejad, A. Langlois, S. Chapuis, B. Michel, W. Faraj, Solar heat injection into boreholes, Proceedings of the 4th Canadian Solar Buildings Conference (2009) 25–27.

[8] A. D. Chiasson, C. Yavuzturk, W. J. Talbert, Design of school building hvac retrofit with hybrid geothermal heat-pump system, Journal of Architectural Engineering 10 (3) (2004) 103–111. doi:10.1061/(ASCE)1076-0431(2004)10:3(103).

[9] H. Biglarian, M. H. Saidi, M. Abbaspour, Economic and environmental assessment of a solar-assisted ground source heat pump system in a heating-dominated climate, International Journal of Environmental Science and Technology 16 (7) (2019) 3091–3098. doi:10.1007/s13762-018-1673-3.
URL https://doi.org/10.1007/s13762-018-1673-3

[10] G. Nouri, Y. Noorollahi, H. Yousefi, Designing and optimization of solar assisted ground source heat pump system to supply heating, cooling and hot water demands, Geothermics 82 (2019) 212 – 231. doi:https://doi.org/10.1016/j.geothermics.2019.06.011.

[11] A. Michopoulos, V. Voulgari, A. Tsikaloudaki, T. Zachariadis, Evaluation of ground source heat pump systems for residential buildings in warm mediterranean regions: the example of cyprus, Energy Efficiency 9 (6) (2016) 1421–1436. doi:10.1007/s12053-016-9431-1.

[12] S. J. Self, B. V. Reddy, M. A. Rosen, Geothermal heat pump systems: Status review and comparison with other heating options, Applied Energy 101 (2013) 341 – 348, sustainable Development of Energy, Water and Environment Systems. doi:https://doi.org/10.1016/j.apenergy.2012.01.048.
URL http://www.sciencedirect.com/science/article/pii/S0306261912000542

[13] A. Omu, S. Hsieh, K. Orehounig, Mixed integer linear programming for the design of solar thermal energy systems with short-term storage, Applied Energy 180 (2016) 313 – 326. doi:https://doi.org/10.1016/j.apenergy.2016.07.055.

[14] S. Miglani, K. Orehounig, J. Carmeliet, Integrating a thermal model of ground source heat pumps and solar regeneration within building energy system optimization, Applied Energy 218 (2018) 78 – 94. doi:https://doi.org/10.1016/j.apenergy.2018.02.173.

[15] Transient system simulation tool (2019) [cited 2020-01-08].
URL http://www.trnsys.com/

[16] Y. J. Nam, X. Y. Gao, S. H. Yoon, K. H. Lee, Study on the performance of a ground source heat pump system assisted by solar thermal storage, Energies 8 (12) (2015) 13378–13394. doi:10.3390/en81212365.

[17] W. Wu, T. You, B. Wang, W. Shi, X. Li, Simulation of a combined heating, cooling and domestic hot water system based on ground source absorption heat pump, Applied Energy 126 (2014) 113 – 122. doi:https://doi.org/10.1016/j.apenergy.2014.04.006.

[18] L. Xia, Z. Ma, G. Kokogiannakis, Z. Wang, S. Wang, A model-based design optimization strategy for ground source heat pump systems with integrated photovoltaic thermal collectors, Applied Energy 214 (2018) 178 – 190. doi:https://doi.org/10.1016/j.apenergy.2018.01.067.
URL http://www.sciencedirect.com/science/article/pii/S0306261918300758

[19] L. Trigeorgis, A. E. Tsekrekos, Real options in operations research: A review, European Journal of Operational Research 270 (1) (2018) 1 – 24. doi:https://doi.org/10.1016/j.ejor.2017.11.055.
URL http://www.sciencedirect.com/science/article/pii/S0377221717310664

[20] F. Longstaff, E. Schwartz, Valuing american options by simulation: A simple least-squares approach, Review of Financial Studies 14 (2001) 113–47. doi:10.1093/rfs/14.1.113.

[21] H. Weeratunge, J. d. Hoog, S. Dunstall, G. Narsilio, S. Halgamuge, Life cycle cost optimization of a solar assisted ground source heat pump system, in: 2018 IEEE Power Energy Society General Meeting (PESGM), 2018, pp. 1–5. doi:10.1109/PESGM.2018.8586063.

[22] H. Weeratunge, G. Narsilio, J. de Hoog, S. Dunstall, S. Halgamuge, Model predictive control for a solar assisted ground source heat pump system, Energy 152 (2018) 974 – 984. doi:https://doi.org/10.1016/j.energy.2018.03.079.

[23] G. R. Aditya, Shallow geothermal systems: individual and district applications, Ph.D. thesis, The university of Melbourne (2020).
URL http://hdl.handle.net/11343/239209

[24] H. Weeratunge, Optimization of sustainable residential heating and cooling systems, Ph.D. thesis, The university of Melbourne (2020).
URL http://hdl.handle.net/11343/242270

[25] S. Li, K. Dong, J. Wang, X. Zhang, Long term coupled simulation for ground source heat pump and underground heat exchangers, Energy and Buildings 106 (2015) 13 – 22, sI: IEA-ECES Annex 31 Special Issue on Thermal Energy Storage. doi:https://doi.org/10.1016/j.enbuild.2015.05.041.
URL http://www.sciencedirect.com/science/article/pii/S0378778815300165

[26] A. Araújo, V. Pereira, Solar thermal modeling for rapid estimation of auxiliary energy requirements in domestic hot water production: On-off flow rate control, Energy 119 (2017) 637 – 651. doi:https://doi.org/10.1016/j.energy.2016.11.025.
URL http://www.sciencedirect.com/science/article/pii/S0360544216316310

[27] H. Li, H. Yang, Potential application of solar thermal systems for hot water production in hong kong, Applied Energy 86 (2) (2009) 175 – 180, iGEC III. doi:https://doi.org/10.1016/j.apenergy.2007.12.005.

[28] X. Gong, L. Wei, W. Feng, Theoretical investigation of operating control strategy of a new solar-water-assisted ground-source heat pump, 2012, pp. 383 –389. doi:10.1201/b13165-80.

[29] Y. Ma, F. Borrelli, B. Hencey, A. Packard, S. Bortoff, Model predictive control of thermal energy storage in building cooling systems, in: Proceedings of the 48h IEEE Conference on Decision and Control (CDC) held jointly with 2009 28th Chinese Control Conference, 2009, pp. 392–397. doi:10.1109/CDC.2009.5400677.

[30] D. Steen, M. Stadler, G. Cardoso, M. Groissböck, N. DeForest, C. Marnay, Modeling of thermal storage systems in milp distributed energy resource models, Applied Energy 137 (2015) 782 – 792. doi:https://doi.org/10.1016/j.apenergy.2014.07.036.
URL http://www.sciencedirect.com/science/article/pii/S0306261914007181

[31] Q. Lu, G. A. Narsilio, G. R. Aditya, I. W. Johnston, Economic analysis of vertical ground source heat pump systems in melbourne, Energy 125 (2017) 107 – 117. doi:https://doi.org/10.1016/j.energy.2017.02.082.

[32] P. E. Hayward, Jenny; Graham, Electricity generation technology cost projections: 2017-2050. newcastle, n.s.w.: Csiro;doi:https://doi.org/10.4225/08/5a3953c5385c3.

[33] D. o. t. E. Australian National Greenhouse Accounts, A. Energy, National greenhouse accounts factors (2017).

[34] Energyplus, the building energy simulation tool developed by us department of energy [cited 2020-01-08].
URL https://energyplus.net/

[35] B. Cao, Y. Zhu, Q. Ouyang, X. Zhou, L. Huang, Field study of human thermal comfort and thermal adaptability during the summer and winter in beijing, Energy and Buildings 43 (5) (2011) 1051 – 1056, tackling building energy consumption challenges - Special Issue of ISHVAC 2009, Nanjing, China. doi:https://doi.org/10.1016/j.enbuild.2010.09.025.

[36] N. Zhang, B. Cao, Z. Wang, Y. Zhu, B. Lin, A comparison of winter indoor thermal environment and thermal comfort between regions in europe, north america, and asia, Building and Environment 117 (2017) 208 – 217. doi:https://doi.org/10.1016/j.buildenv.2017.03.006.

[37] Australian energy council.

[38] [cited 2019-05-20][link].
URL https://www.statista.com/statistics/263492/electricity-prices-in-selected-countries/

[39] International energy agency [cited 2019-05-20].
URL https://www.iea.org/statistics/kwes/prices/

[40] M. Brander, A. Sood, C. Wylie, A. Haughton, J. Lovell, Electricity-specific emission factors for grid electricity, Ecometrica.

Appendix A. Parameters

Table A.3: Parameters

Heat pump fluid	water
Specific heat capacity of the fluid C_p	4200 $JK^{-1}kg^{-1}$
Density of the fluid ρ	1000 kgm^{-3}
Borehole radius r_b	0.07 m
Equivalent pipe radius $r_{p,eq}$	25 mm
*Borehole thermal resistance R_b	0.035 mKW^{-1}
*Grout thermal conductivity λ_b	2.03 $WK^{-1}m^{-1}$
*Ground thermal diffusivity α	2.53 $\times 10^{-3} m^2h^{-1}$
*Ground thermal conductivity λ	1.90 $WK^{-1}m^{-1}$
Storage tank volume V^s	0.3 m^3
*Installation cost of the tank	$ 1362
*Average cost of drilling	$ 139.45 per meter
*Cost of the ground source heat pump	$ 6580
*Other costs related to GSHP installation	$ 8860
*Average installation cost of solar collectors	$ 547 per m^2
*Installation cost of ASHP system	$ 8481
Cooling efficiency of ASHP system	2.5
*Installation cost of gas furnace	$ 4203
*Heating efficiency of gas furnace	76%
*Electricity inflation	6.2%
*Gas Inflation	6.14%
*Minimum attractive rate of return	3.5%
*Consumer price index	2.58 %
Solar collector life span	20 years
CO_2 emission factor for gas	0.185 kg per kWh

*Parameters obtained from Melbourne

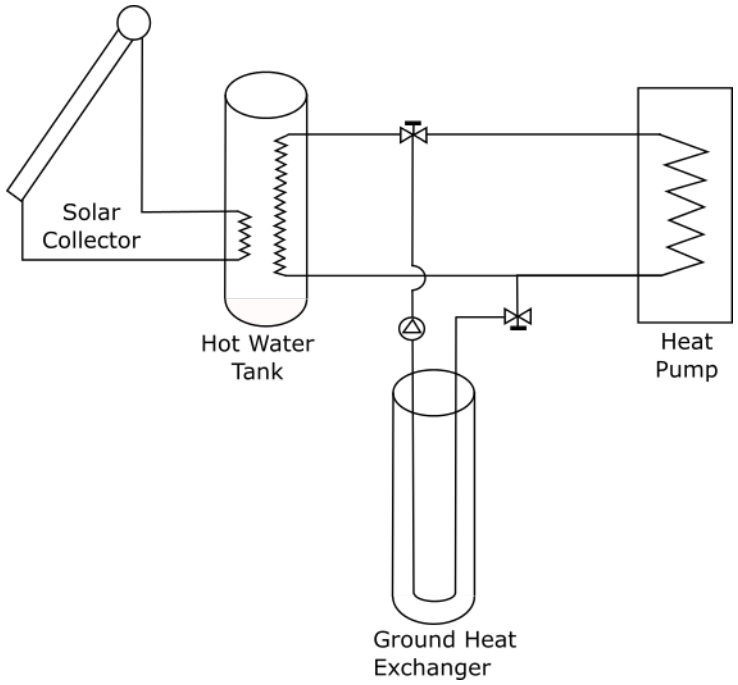

Figure B.18: Schematic of the SAGSHP system

Appendix B. Instrumentation and Data Collection

There are 23 GSHP systems installed in metropolitan Melbourne as part of the Sustainable Energy Pilot Demonstration (SEPD). One of these properties located in Footscray was modified to a Solar Assisted GSHP system due to its low performance during winter. 30 evacuated tube collectors and a thermal storage tank with double heat exchangers were combined to the GSHP. A detail description of the SEPD project, instrumentation and data collection can be found in [23]. However, this Appendix provides a summary of the instrumentation and data collection of the SAGSHP system installation in Footscray, Victoria, Australia.

A schematic of the system considered in this study is presented in Figure **??**. This system consist of a GHE with depth of $110m$, evacuated tube solar collectors with 30 tubes, and a $300L$ thermal storage.

In the experiment, temperatures, flow rates of the circulation fluid and the power consumption of the heat pump was collected in five minutes interval over sixteen months. The following subsections describes the parameters monitored and the instrumentation used.

Appendix B.1. Temperature Measurements

Negative temperature coefficient (NTC) thermistors from EmersonTM has been used to measure the temperatures of the systems at the following locations. Thermistors are attached to copper pipes before the insulation is installed.

- Temperature of the water entering and exiting the GSHP
- Temperature of the inlet and outlet of the solar collectors
- Temperatures of the inlet and the outlet of the tank to the ground loop
- Temperature of the tank at two node points

Figure B.19: Solar thermal collectors

Figure B.20: Thermal storage tank

Figure B.21: Temperature measurement of the thermal storage tank

The temperature of the two node points has been monitored as shown in the Figure A.4. The top node has been connected to the data logger for the purpose of data collection, and the mid level sensor was connected to the controller.

Appendix B.2. Flow rate

A flow meter has been used to measure the flow rate of the ground loop. This is an important parameter to that is required to calculate the amount of energy transferred from the ground to the building.

Appendix B.3. Electricity Consumption

The electricity consumption of the system was measured by a power meter. This includes the energy consumed by the heat pump and the fluid circulation pump of the system.